Chinese Chemical Letters 37 (2026) 111146

Contents lists available at ScienceDirect

Chinese Chemical Letters

journal homepage: www.elsevier.com/locate/cclet

Preparation of a homochiral metal-organic cage and its bonded silicas for efficient enantioseparation in high-performance liquid chromatography and gas chromatography

Jun-Hui Zhang*, Rui-Xue Liang, Bin Huang, Li-Qin Yu, Juan Chen, Bang-Jin Wang*, Sheng-Ming Xie*, Li-Ming Yuan

Yunnan Key Laboratory of Modern Separation Analysis and Substance Transformation, College of Chemistry and Chemical Engineering, Yunnan Normal University, Kunming 650500, China

ARTICLE INFO

Article history:
Received 17 July 2024
Revised 7 February 2025
Accepted 26 March 2025
Available online 26 March 2025

Keywords:
Chiral metal-organic cage
Chiral stationary phase
Chiral separation
High-performance liquid chromatography
Gas chromatography

ABSTRACT

Developing a chiral material as versatile and universal chiral stationary phase (CSP) for chiral separation in diverse chromatographic techniques simultaneously is of great significance. In this study, we demonstrated for the first time that a chiral metal-organic cage (MOC), $[Zn_6M_4]$, as a universal chiral recognition material for both multi-mode high-performance liquid chromatography (HPLC) and capillary gas chromatography (GC) enantioseparation. Two novel HPLC CSPs with different bonding arms (CSP-A with a cationic imidazolium bonding arm and CSP-B with an alkyl chain bonding arm) were prepared by clicking of functionalized chiral MOC $[Zn_6M_4]$ onto thiolated silica *via* thiol-ene click chemistry. Meanwhile, a capillary GC column statically coated with the chiral MOC $[Zn_6M_4]$ was also fabricated. The results showed that the chiral MOC exhibits excellent enantioselectivity not only in normal phase HPLC (NP-HPLC) and reversed phase (RP-HPLC) but also in GC, and various racemates were well separated, including alcohols, diols, esters, ketones, ethers, amines, and epoxides. Importantly, CSP-A and CSP-B are complementary to commercially available Chiralcel OD-H and Chiralpak AD-H columns in enantioseparation, which can separate some racemates that could not be or could not well be separated by the two widely used commercial columns, suggesting the great potential of the two prepared CSPs in enantioseparation. This work reveals that the chiral MOC is potential versatile chiral recognition materials for both HPLC and GC, and also paves the way to expand the potential applications of MOCs.

© 2025 Published by Elsevier B.V. on behalf of Chinese Chemical Society and Institute of Materia Medica, Chinese Academy of Medical Sciences.

The separation of enantiomers is of great significance in many industries, particularly in pharmaceutical industry, because many drugs are chiral and different enantiomers of a chiral drugs will exhibit distinct biological and pharmacological effects in organisms [1,2]. Among of various chiral resolution methods, chromatographic techniques rely on chiral stationary phases (CSPs), such as high-performance liquid chromatography (HPLC) and gas chromatography (GC), have been considered to be the most popular methods for the separation of enantiomers [3,4]. To date, diverse chiral materials, such as cyclodextrins [5–8], polysaccharides [3,9–11], chiral crown ethers [12], amino acid derivatives [13], and metal complexes [14,15], have been explored as CSPs for HPLC and GC. However, each CSP has more or less shortcomings, such as limited chiral separation ability, complex preparation process, high cost, unsatisfied stability, and narrow applicability. Moreover, there are also few chiral materials that can be simultaneously used for multi-mode HPLC and GC enantioseparation with good enantioselectivity. For example, cellulose tris(3,5-dimethylphenylcarbamate) (commercial Chiralcel OD) is one of the most popular chiral materials and exhibits outstanding chiral separation capability in NP-HPLC, whereas it gives almost no enantioselectivity in GC and an obvious decrease chiral separation capability in RP-HPLC [3,10]. Permethylated β-cyclodextrin is a superior and widely used GC CSP, but its enantioselectivity is low in HPLC [5]. Similarly, chiral crown ethers show good enantioselectivity in HPLC, but almost no enantioselectivity in GC. Most chiral crown ethers and cyclodextrins-based CSPs are generally used for enantioseparation

* Corresponding authors.
E-mail addresses: zjh19861202@126.com (J.-H. Zhang), wangbangjin711@163.com (B.-J. Wang), xieshengming_2006@163.com (S.-M. Xie).

https://doi.org/10.1016/j.cclet.2025.111146
1001-8417/© 2025 Published by Elsevier B.V. on behalf of Chinese Chemical Society and Institute of Materia Medica, Chinese Academy of Medical Sciences.

in RP-HPLC, but rarely used in NP-HPLC. Therefore, developing versatile and universal CSPs that can be simultaneously used for enantioseparation in diverse chromatographic techniques is still the research focus.

During the past decade, many novel porous materials, including metal-organic frameworks (MOFs) [16–19], covalent organic frameworks (COFs) [20–24], and porous organic polymers (POPs) [25,26], have been widely used as stationary phases for chromatographic separations and aroused considerable research interest due to their features of large surface areas, well-defined and ordered pores, and diverse topological structures. However, such porous frameworks are insoluble in organic solvents. Therefore, there are some difficulties and inconveniences in preparing uniform stationary phases and high efficiency columns, which had limited their applications and superior performances in some case. For example, they cannot be dissolved in solvents to form homogeneous solutions caused hard to immobilize or coat onto chromatographic matrices through chemical reactions to prepare pressure resistant and uniform HPLC stationary phases, thus most of applications in HPLC involve directly pack irregular particles of MOFs or COFs [19,22], which often give low column efficiency and high column pressure. Even if they are immobilized on the chromatographic matrices to prepare core-shell composite materials as stationary phases through *in-situ* growth methods, there are still difficulties in controlling the uniformity and thickness of the prepared shell layer. Meanwhile, when they were used as GC stationary phases, their particle suspensions were coated by a dynamic coating method to prepare capillary GC columns, while overwhelming majority of commercial capillary GC columns with good reproducibility are prepared by the static coating method.

Metal-organic cages (MOCs), also known as metal-organic polyhedrons (MOPs) or porous coordination cages (PCCs), are an emerging class of supramolecular porous materials constructed by coordination driven self-assembly of metal ions and organic linkers [27–29]. Comparing with porous frameworks, such as MOFs and COFs, MOCs are discrete, cage-like coordination assemblies which can be self-assembled into supramolecular porous solids through weak intermolecular forces rather than robust chemical bonds (covalent or coordination bonds). Therefore, one of the biggest differences between MOCs and framework materials (*e.g.*, MOFs and COFs) is that MOCs are porous molecular materials with good solubility, which can be soluble in some organic solvents without changing structures. The good solubility of MOCs imbues them have excellent solution processability [30–32]. For instance, in homogeneous solution, MOCs can be more effective and easier to modify structures undergo various chemical reactions and to immobilize onto uniform matrices to prepare chromatographic separation materials. By contrast, the post-modification and functionalization of MOFs and COFs only can be conducted in their heterogeneous solid suspensions, which have unsatisfactory and incomparable post-modification effects to MOCs. The unique features of MOCs including good solubility, excellent solution processability, and accessible internal cavities, which also make them a good application prospect in molecular recognition [33–35], separation [36–39], catalysis [40], sensing [35,41,42], and biomedical [43]. In 2018, our group first reported the use of a homochiral MOC as CSP for enantioseparation in GC [44], demonstrating the great potential of chiral MOCs for chiral separation in chromatography. Subsequently, some chiral MOCs were also explored as CSPs for GC [45,46]. However, the application of MOCs as CSPs for HPLC enantioseparation has been reported rarely so far.

In this study, we reported the first immobilization of a chiral octahedral MOC [Zn_6M_4] onto chromatographic silica *via* thiol-ene click chemistry to construct two novel CSPs (CSP-A and CSP-B) with different bonding arms for HPLC enantioseparation. Meanwhile, the [Zn_6M_4] was also used as CSP and statically coated on a capillary column to fabricate a GC column for enantioseparation. The chiral MOC [Zn_6M_4] was synthesized by coordination self-assembly of six Zn^{2+} with four trianglsalen macrocycles (M) (Fig. 1) [47,48]. Then, it was immobilized onto thiolated silica (SiO_2-SH) *via* thiol-ene click chemistry to prepare CSP-A and CSP-B (Fig. 2). ^{1}H NMR, ^{13}C NMR, fourier translation infrared (FT-IR), MALDI-TOF-MS, and powder X-ray diffraction (PXRD) confirm the successful synthesis of [Zn_6M_4] (Figs. S3 and S4 in Supporting information). N_2 adsorption and desorption isotherms and pore size distribution data of the [Zn_6M_4] have been provided in Fig. S5 (Supporting information). The Brunauer-Emmett-Teller (BET) surface area of the [Zn_6M_4] is 796 m^2/g, and the pore size distribution is primarily centered at 11 Å. Thermogravimetric analysis (TGA) indicates that there is no significant weight loss of [Zn_6M_4] crystals before 350 °C, suggesting that it has good thermal stability when used as a GC stationary phase.

Scanning electron microscopy (SEM), X-ray photoelectron spectroscopy (XPS), FT-IR, TGA, and elemental analysis (EA) were used to demonstrate the successful preparation of CSP-A and CSP-B. SEM images reveal that the surface of SiO_2-SH is smooth, whereas the surfaces of CSP-A and CSP-B are loaded with many solids ([Zn_6M_4]) (Fig. S6 in Supporting information). As shown in Fig. S7 (Supporting information), compared to SiO_2-SH, the emergence of Zn 2p and N 1s signal peaks in the XPS spectra of CSP-A and CSP-B indicates the immobilization of [Zn_6M_4] on the SiO_2-SH surface. Furthermore, Br 3d signal peak also appears in the XPS spectrum of CSP-A. In FT-IR spectrum (Fig. 3a), by comparison with SiO_2-SH, the increase of C=N characteristic bands at $\nu = 1608$ cm^{-1} and saturated C–H bands at $\nu = 2930$ and 2857 cm^{-1} in CSP-A and CSP-B, and the appearance of new absorptions at ν = 1474 and 1367 cm^{-1} in CSP-A and CSP-B, which confirm the successful clicking of [Zn_6M_4] onto SiO_2-SH. Moreover, the weight loss of CSP-A and CSP-B is more obvious in comparison with SiO_2-SH due to the decomposition of the organic components of [Zn_6M_4] bonded onto the SiO_2-SH (Fig. 3b). The EA data show that the C, H, and N contents in CSP-A and CSP-B were significantly increased compared to SiO_2-SH (Table S1 in Supporting information), further proving the successful clicking of [Zn_6M_4] onto SiO_2-SH. According to Eq. S1 (Supporting information), the surface bonding amount of CSP-A and CSP-B were calculated to be 0.08 and 0.07 μmol/m^2, respectively. The number of theoretical plates calculated with benzene under normal phase conditions was 18,500 plates/m for CSP-A packed column A and 16,900 plates/m for CSP-A packed column B. Similarly, calculated with naphthalene under reversed phase conditions, the numbers were 16,200 plates/m for column A and 15,800 plates/m for column B.

SEM images displayed that the [Zn_6M_4] was uniformly coated on the inner surface of the capillary column with a coating thickness of about 226 nm (Fig. S8 in Supporting information). The column efficiency of the capillary GC column is 3100 plates/m by determining *n*-dodecane on the GC column at 120 °C (Fig. S9 in Supporting information). Table S2 (Supporting information) gives the McReynolds constants of five representative analytes on the GC column. The average McReynolds constants of the five analytes was 213, revealing a moderate polarity of the GC column.

To investigate the enantioseparation capability of CSP-A and CSP-B in NP-HPLC, different types of enantiomers were separated on the two fabricated HPLC columns using *n*-hexane/isopropanol (*n*-HEX/*i*-PrOH) as mobile phase. For CSP-A packed column A, 9 racemates were separated ($\alpha > 1.0$) (Fig. 4a and Table S3 in Supporting information). Among which, 8 racemates achieved baseline separation ($Rs > 1.5$) (Fig. 4b and Table S3), and some racemates obtained high *Rs*, such as 1-(4-fluorophenyl)ethanol ($Rs = 3.36$), ethyl mandelate ($Rs = 3.15$), and 2–methoxy-2-phenylethanol ($Rs = 2.63$). Figs. 5a-c and Fig. S10 (Supporting information) are the chromatograms obtained on col-

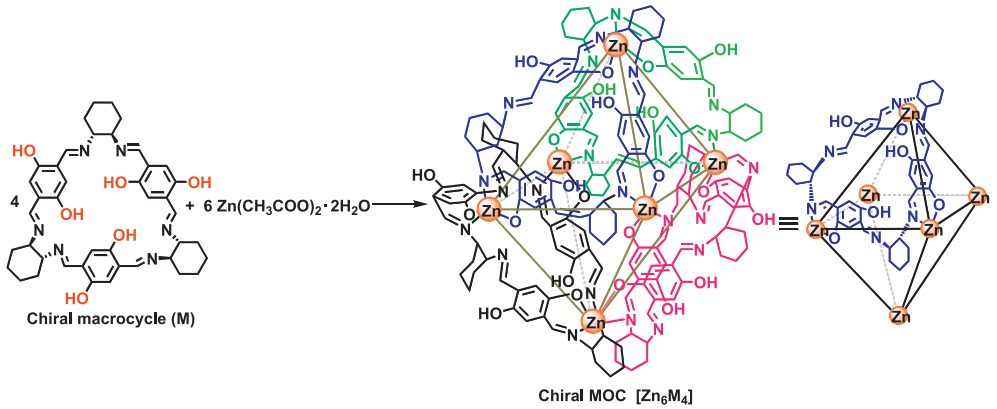


Fig. 1. Synthesis of chiral MOC [Zn_6M_4].

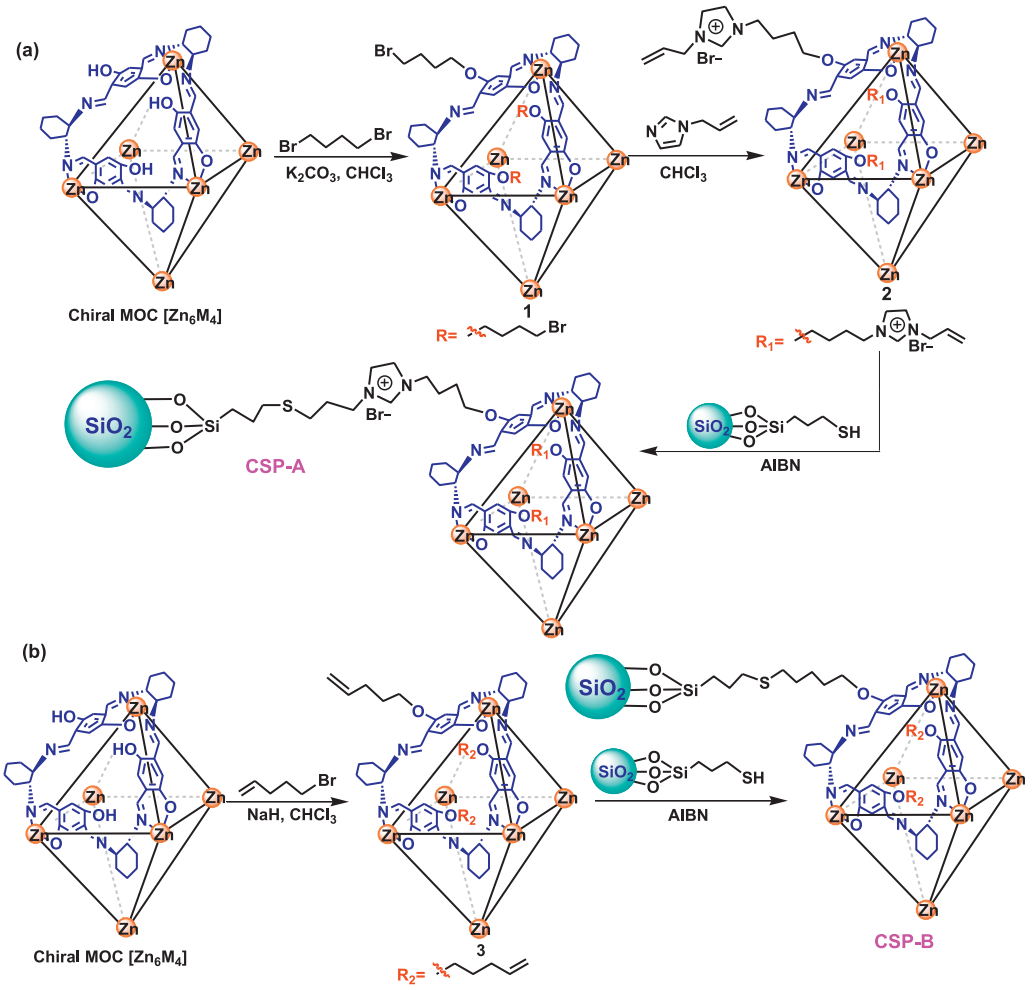


Fig. 2. Preparation of [Zn_6M_4]-based CSP-A (a) and CSP-B (b).

umn A. On CSP-B packed column B, 9 racemates were separated (Fig. 4a and Table S3) and 5 racemates achieved baseline separation (Fig. 4b and Table S3), and high resolutions of benzoin ($Rs = 4.16$) and 4,4′-dimethylbenzoin ($Rs = 2.32$) were achieved. Figs. 5d-f and Fig. S11 (Supporting information) present the separation chromatograms obtained on column B. Analyzing Table S3, it can be found that 6 racemates (benzoin, 4,4′-dimethylbenzoin, 1-(3-fluorophenyl)ethanol, methyl mandelate, 4-chlorobenzhydrol, and 4-methylbenzhydrol) cannot be separated on column A, but can be separated on column B. Meanwhile, 6 racemates (1-(4-fluorophenyl)ethanol, 2–methoxy-2-phenylethanol, 1-phenyl-1-pentanol, 1-(3-bromophenyl)ethanol, 1-(4-bromophenyl)ethanol, and 1-phenylethanol) cannot be separated on column B, but can achieve good separation on column A. Comparing columns A and B, 3 racemates (ethyl mandelate, styrene oxide, and 1-(4-chlorophenyl)ethanol) can be separated on both two prepared columns. Therefore, the [Zn_6M_4]-based two CSPs with different bonding arms exhibit different chiral separation effects, and they

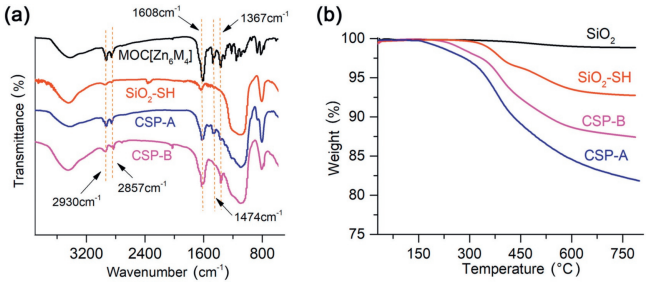


Fig. 3. (a) FT-IR spectra of chiral MOC [Zn_6M_4], SiO_2-SH, CSP-A, and CSP-B. (b) TGA curves of silica (SiO_2), SiO_2-SH, CSP-A, and CSP-B.

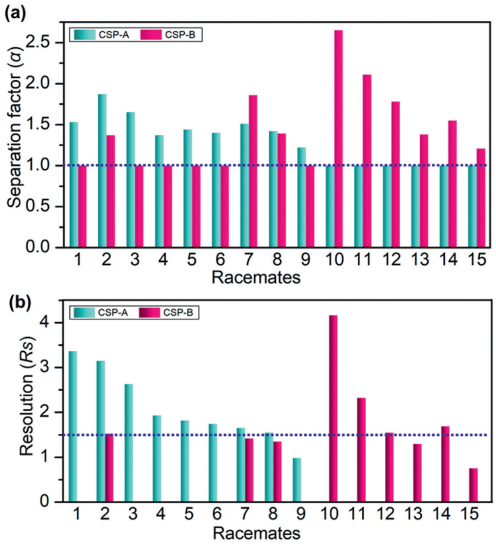


Fig. 4. Statistical data for the separation of racemates on CSP-A and CSP-B in NP-HPLC. (a) The α values of racemates separated on CSP-A and CSP-B. (b) The *Rs* values of racemates separated on CSP-A and CSP-B. 1: 1-(4-fluorophenyl)ethanol; 2: ethyl mandelate; 3: 2–methoxy-2-phenylethanol; 4: 1-phenyl-1-pentanol; 5: 1-(3-bromophenyl)ethanol; 6: 1-(4-bromophenyl)ethanol; 7: styrene oxide; 8: 1-(4-chlorophenyl)ethanol; 9: 1-phenylethanol; 10: benzoin; 11: 4,4′-dimethylbenzoin; 12: 1-(3-fluorophenyl)ethanol; 13: methyl mandelate; 14: 4-chlorobenzhydrol; 15: 4-methylbenzhydrol.

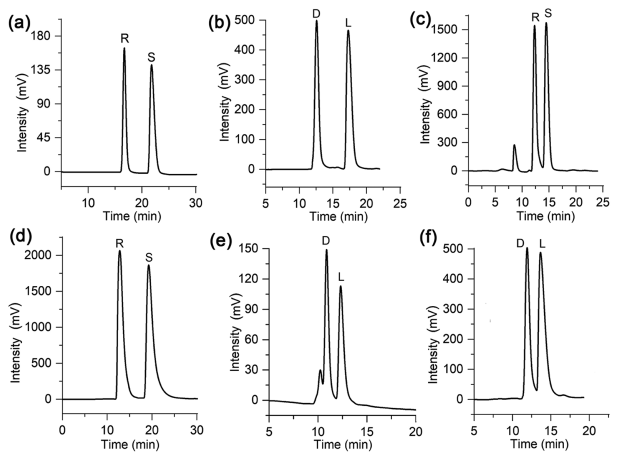


Fig. 5. Representative chromatograms obtained on column A (packed with CSP-A) under NP-HPLC: (a) 1-(4-fluorophenyl)ethanol, (b) ethyl mandelate, (c) 1-(4-chlorophenyl)ethanol. Representative chromatograms obtained on column B (packed with CSP-B) under NP-HPLC: (d) 4,4′-dimethylbenzoin, (e) ethyl mandelate, (f) methyl mandelate.

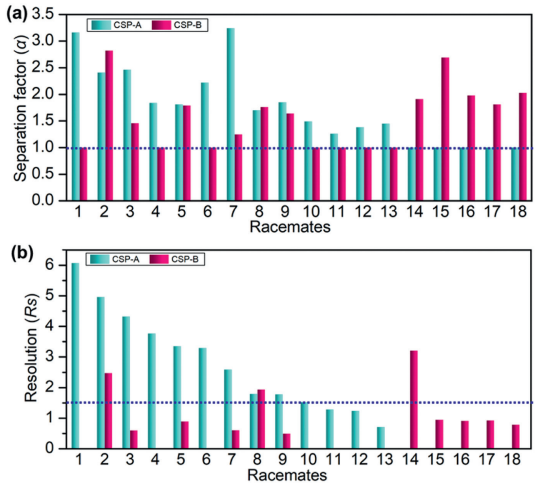


Fig. 6. Statistical data for the separation of racemates on CSP-A and CSP-B in RP-HPLC. (a) The α values of racemates separated on CSP-A and CSP-B. (b) The *Rs* values of racemates separated on CSP-A and CSP-B. 1: piperoin; 2: anisoin; 3: 4,4′-dimethylbenzoin; 4: 1-(4-methylphenyl)ethanol; 5: 1-phenyl-1-pentanol; 6: benzoin; 7: zopiclone; 8: 1-phenylethanol; 9: 2–methoxy-2-phenylethanol; 10: 1-(4-fluorophenyl)ethanol; 11: benzoin ethyl ether; 12: methyl mandelate; 13: 1-phenyl-1-butanol; 14: 2-phenylcyclohexanone; 15: 4-methylbenzhydrol; 16: 4-fluoro-α-methylbenzylamine; 17: ethyl mandelate; 18: 3-benzyloxy-1,2-propanediol.

are complementary to each other in enantioseparation under NP-HPLC, thus the separation range and applicability of the [Zn_6M_4]-based columns are broadened.

Separations of the above tested 15 racemates were also carried out on commercially available Chiralcel OD-H and Chiralpak AD-H columns for comparison. The enantioseparation data and comparative chromatograms are presented in Table S3 and Fig. S12 (Supporting information). It can be found that 5 racemates (1-(4-fluorophenyl)ethanol, 1-phenyl-1-pentanol, styrene oxide, 1-(3-fluorophenyl)ethanol, and 4-chlorobenzhydrol) cannot be enantioseparated on Chiralcel OD-H column; and 5 racemates (1-(4-fluorophenyl)ethanol, 1-phenyl-1-pentanol, 1-(3-bromophenyl)ethanol, 1-phenylethanol, and 1-(3-fluorophenyl)ethanol) cannot be separated on Chiralpak AD-H column. Moreover, some racemates were separated with higher α and *Rs* on the two fabricated columns than those on Chiralcel OD-H or Chiralpak AD-H columns. In addition, 3 racemates, including 1-(4-fluorophenyl)ethanol, 1-phenyl-1-pentanol, and 1-(3-fluorophenyl)ethanol neither can be enantioseparated on Chiralcel OD-H nor can be enantioseparated on Chiralpak AD-H. The mobile phase for separating each racemate on the two commercial columns was not thoroughly optimized, which is the most frequently used and recommended. Of course, some changes in the composition of the mobile phase can lead to some variations in chromatographic performance. By adjusting the composition of the mobile phase, it may be possible to achieve better separation of some racemates. Therefore, the two fabricated columns (column A and column B) can separate some chiral compounds that cannot be separated or only partially separated on the two commercial columns, which are also complementary to the two commercial columns in chiral separation and have potential application prospect.

The enantioseparation capability of CSP-A and CSP-B were also assessed in RP-HPLC using MeOH/H_2O as mobile phase. In Table S4 (Supporting information) and Fig. 6, a total of 13 racemates achieved enantioseparation ($\alpha > 1.0$) on column A (Fig. 6a), and most of racemates achieved baseline separation (*Rs* > 1.5) except 3 racemates of benzoin ethyl ether, methyl mandelate, and 1-phenyl-1-butanol (Fig. 6b). High res-

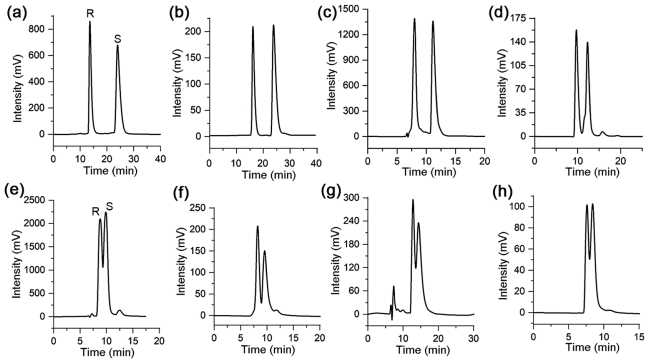


Fig. 7. Representative chromatograms obtained on column A (packed with CSP-A) under RP-HPLC: (a) 4,4′-dimethylbenzoin, (b) 1-phenyl-1-pentanol, (c) zopiclone, (d) 2–methoxy-2-phenylethanol. Representative chromatograms obtained on column B (packed with CSP-B) under RP-HPLC: (e) 4,4′-dimethylbenzoin, (f) 1-phenyl-1-pentanol, (g) zopiclone, (h) 2–methoxy-2-phenylethanol.

olution of many racemates were achieved, such as piperoin ($Rs = 6.07$), anisoin ($Rs = 4.96$), 4,4′-dimethylbenzoin ($Rs = 4.32$), and 1-(4-methylphenyl)ethanol ($Rs = 3.77$). For column B, 11 racemates obtained enantioseparation ($\alpha > 1.0$) (Fig. 6a), of which 3 racemates (anisoin, 1-phenylethanol, and 2-phenylcyclohexanone) achieved baseline separation ($Rs > 1.5$) (Table S4 and Fig. 6b). Fig. 7 shows some representative chromatograms for the separation racemates on columns A and B. Other chromatograms for the separation of racemates on columns A and B are provided in Figs. S13 and S14 (Supporting information), respectively. Moreover, 5 racemates, including 2-phenylcyclohexanone, 4-methylbenzhydrol, 4-fluoro-α-methylbenzylamine, ethyl mandelate, and 3-benzyloxy-1,2-propanediol, cannot be enantioseparated on column A but can be enantioseparated on column B, while 7 racemates, including piperoin, 1-(4-methylphenyl)ethanol, benzoin, 1-(4-fluorophenyl)ethanol, benzoin ethyl ether, methyl mandelate, and 1-phenyl-1-butanol, cannot be enantioseparated on column B but can be enantioseparated on column A (Table S4 and Fig. 6). In addition, six racemates, including anisoin, 4,4′-dimethylbenzoin, 1-phenyl-1-pentanol, zopiclone, 1-phenylethanol, and 2–methoxy-2-phenylethanol, could be enantioseparated on both columns A and B (Table S4 and Fig. 6). Among these 18 racemates separated by column A and column B, 5 racemates cannot be separated by Chiralpak OD-H column, while 8 racemates cannot be separated by Chiralpak AD-H column (Table S4). The obtained chromatograms on the four columns are compared in Fig. S15 (Supporting information). From the above experimental results, it can be seen that CSP-A and CSP-B also have excellent chiral recognition ability and complementary to each other under reversed phase condition.

The chiral MOC [Zn_6M_4] shows octahedron shape and large intrinsic cavity with eight pore windows, which was constructed by coordination of four chiral macrocycle (M) with six Zn^{2+} (Fig. 2 and Fig. S16a in Supporting information) [48]. Each cage molecule has eight pore windows which can be divided into two types. Four pore windows from the four used chiral macrocycle (M) themselves (Fig. S16b in Supporting information), the area with green circle). Another four pore windows formed by the connection of three neighbouring chiral macrocycles (M) with three Zn^{2+} (the area with pink circle, Fig. S16c in Supporting information). The intrinsic cavity in each [Zn_6M_4] molecule is a good place to accommodate guests. Analytes can access to the intrinsic cavity through the pore windows and host-guest interactions will occur with the chiral MOP [Zn_6M_4], which are vital important for chiral separation. Furthermore, there are many hydrogen bonding sites (*e.g.*, O and N atoms) in the [Zn_6M_4], and many racemates with hydrogen bond donors (such as alcohols and amines) were well enantioseparated, indicating that hydrogen bonding interaction also plays a significant role in enantioseparation. In a word, the excellent enantioselectivity of [Zn_6M_4] is largely due to its unique molecular structure, such as cage-like structure with intrinsic cavity, various active sites (hydrogen bonding sites, benzene rings, Zn^{2+} metal center), by which host-guest inclusion, hydrogen bonding, weak coordination, π-π, and dipole-dipole interactions play key roles in enantioseparation.

It is known that the bonding arm may affect chiral separation in some cases. Compared to CSP-B, CSP-A features a cationic imidazolium bonding arm. The presence of cationic imidazolium can provide additional interactions between CSPs and analytes, such as electrostatic, π-π, and hydrophilic/hydrophobic interactions, which are crucial for chiral separation [49–52]. CSP-A exhibits better separation for some racemates than CSP-B, especially under reversed-phase conditions, because the cationic imidazolium spacers can provide strong hydrophobic, electrostatic, and π-π interactions, thereby endowing it with better separation ability than CSP-B in reversed-phase mode. For example, many hydrophilic alcohols (*e.g.*, 1-phenyl-1-pentanol, 2–methoxy-2-phenylethanol, 1-(4-fluorophenyl)ethanol, and piperoin) were better separated on CSP-A than on CSP-B. Fig. 7 also shows the four racemates were better separated on CSP-A than on CSP-B under reversed-phase mode.

Taking the resolution of 1-(4-fluorophenyl)ethanol under NP-HPLC and 1-(4-methylphenyl)ethanol under RP-HPLC on column A as examples, the effects of some factors on enantioseparation were studied, including column temperature, mobile phase composition, and analyte mass. In Figs. S17a and b (Supporting information), it was observed that as the column temperature gradually increased from 20 °C to 40 °C, the *Rs* and retention time of both two analytes decreased significantly, suggesting that the separations are exothermic. The van't Hoff curves exhibit a good linear relationship, indicating no changes on the interaction mechanism at this temperature range (Figs. S17c and d in Supporting information). The values of ΔH, ΔS, and ΔG (Eqs. S2-S4 in Supporting information) are calculated and shown in Table S5 (Supporting information). The ΔG values of *S*-enantiomers of the two analytes are more negative than *R*-enantiomers, indicating that the retention of *S*-enantiomers on the CSP will stronger than *R*-enantiomers, which is consistent with the experimental results (Figs. S17a and b).

Fig. S18 (Supporting information) shows enantioseparations of the two analytes using mobile phase with different compositions. In NP-HPLC, as increase of the polarity of the mobile phase, that is, the content of *i*-PrOH in the mobile phase increased, the retention time and *Rs* of 1-(4-fluorophenyl)ethanol enantiomers gradually reduced. When the content of *i*-PrOH is 1% in mobile phase, 1-(4-fluorophenyl)ethanol has the highest *Rs* value but the longest retention time, while the content of *i*-PrOH increases to 15%, 1-(4-fluorophenyl)ethanol cannot be enantioseparated (Fig. S18a). In RP-HPLC, as the MeOH content increases from 40% to 70%, the retention time and *Rs* of 1-(4-methylphenyl)ethanol enantiomers significantly reduced (Fig. S18b). Therefore, selecting the appropriate mobile phase composition can enhance the enantiomeric separation effect.

The effect of analyte mass on enantioseparation was studied. From Fig. S19 (Supporting information), when the injection masses of the analytes increase from 1 μg to 20 μg, a good linear relationship between the chromatographic peak area and the injection mass were achieved, and the separation effects and retention times remain basically unchanged. When the analyte mass increased to 20 μg, high resolution of the two analytes can also be obtained. This feature of the column make it has potential application prospects in qualitative and quantitative analysis.

The HPLC column also has good stability and reproducibility. After hundreds of injections (100, 200, 300, and 400 injections),

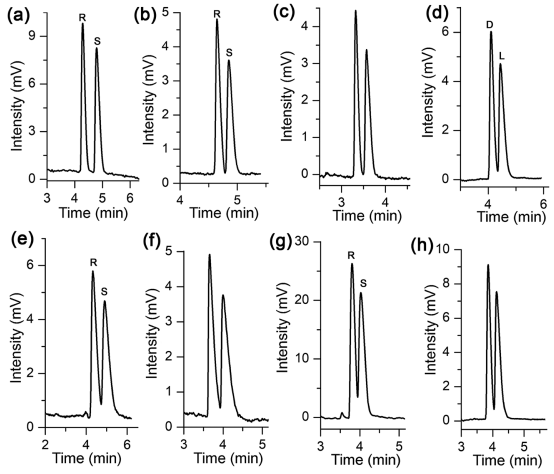


Fig. 8. Representative chromatograms of resolution of racemates on the GC column. (a) γ-Hexalactone, (b) β-butyrolactone, (c) γ-heptalactone, (d) methyl 2-bromopropionate, (e) 2-pentanol, (f) γ-valerolactone, (g) 1-phenylethanol acetate, (h) 2-bromobutanoic acid ethyl ester.

the retention time and *Rs* of the two analytes remained almost unchanged in comparison with its initial of use (Fig. S20 in Supporting information). The RSDs ($n = 5$) of retention time and *Rs* were $<0.65\%$ and 1.20% (Table S6 in Supporting information), respectively.

The enantioselectivity of $[Zn_6M_4]$ as CSP in GC was also investigated. Various chiral compounds were employed as analytes for separating on the fabricated capillary GC column, and 20 racemates have been enantioseparated on the column. The separation conditions and enantioseparation data were presented in Table S7 (Supporting information). The representative chromatograms are shown in Fig. 8. Furthermore, the $[Zn_6M_4]$-coated capillary GC column also shows excellent separation for various types of organic isomers, including positional, *cis-/trans-*, and structural isomers. In Table S8 and Fig. S21 (Supporting information), 6 positional isomers (dichlorobenzene, chloroaniline, nitrotoluene, nitrochlorobenzene, nitrobromobenzene, and xylene), 3 *cis-/trans*-isomers (1,3-dichloropropene, 1,2,3-trichloropropene, and 2,5-dimethoxytetrahydrofuran), and structural isomers of butanol were well separated on the capillary GC column. Among them, baseline separations of most isomers were achieved. The results indicate good selectivity of the $[Zn_6M_4]$-coated GC column in separating racemates and organic isomers.

The reproducibility of the capillary GC column after hundreds of injections was examined using γ-hexalactone and *o,m,p*-dichlorobenzene as analytes. In Fig. S22 (Supporting information), the separation effects of the two analytes were almost unchanged after hundreds of injections (100, 250, and 400 times). The RSDs ($n = 5$) of retention time and *Rs* for analytes separated on the GC column before and after it was undergone different injections of use were $<1.12\%$ and 1.66% (Table S9 in Supporting information), respectively. The thermal stability of the GC column was also determined by separating γ-heptalactone and *o,m,p*-chloroaniline before and after the column has been dealt with 300 °C high temperature. In Fig. S23 (Supporting information), after the column dealt with 300 °C high temperature for 3, 5, and 7 h, the separation effects of the two analytes were almost unchanged compared to the initial use of the column. The RSDs ($n = 5$) of retention time and *Rs* for analytes separated on the GC column before and after it was undergone different times of high temperature treatment were $<1.82\%$ and 1.96% (Table S10 in Supporting information), respectively. The results indicate that the GC column has excellent reproducibility and thermal stability.

In conclusion, we have reported for the first time that the development of a chiral MOC $[Zn_6M_4]$ as versatile CSP for both multimode HPLC and GC enantiomeric separation. The chiral MOC as CSP exhibited excellent enantioselectivity not only in NP-HPLC and RP-HPLC, but also in GC. In NP-HPLC, both CSP-A and CSP-B were able to separate 9 racemates. In RP-HPLC, 13 racemates were well separated on CSP-A, and 11 racemates were separated on CSP-B. In GC, 20 racemates and various organic isomers were separated on the $[Zn_6M_4]$-coated capillary GC column. Importantly, the two prepared HPLC CSPs are also complementary to commercial Chiralcel OD-H and Chiralpak AD-H columns, and can separate some racemates that cannot be enantioseparated or cannot be well enantioseparated by the two commercial columns. The results demonstrate that the chiral MOC is a versatile chiral recognition material for chromatography and has great potential in enantioseparation.

Declaration of competing interest

The authors declare that they have no known competing financial interests or personal relationships that could have appeared to influence the work reported in this paper.

CRediT authorship contribution statement

Jun-Hui Zhang: Writing – review & editing, Writing – original draft, Supervision, Project administration, Investigation, Funding acquisition, Formal analysis. **Rui-Xue Liang:** Investigation, Formal analysis, Data curation, Conceptualization. **Bin Huang:** Validation, Methodology, Investigation, Formal analysis. **Li-Qin Yu:** Software, Data curation, Conceptualization. **Juan Chen:** Visualization, Software, Methodology, Data curation. **Bang-Jin Wang:** Software, Funding acquisition, Formal analysis, Data curation. **Sheng-Ming Xie:** Visualization, Resources, Funding acquisition, Formal analysis. **Li-Ming Yuan:** Resources, Funding acquisition.

Acknowledgments

This work was supported by the National Natural Science Foundation of China (Nos. 22064020, 22364022, and 22174125) and the Applied Basic Research Foundation of Yunnan Province (Nos. 202101AT070101 and 202201AT070029).

Supplementary materials

Supplementary material associated with this article can be found, in the online version, at doi:10.1016/j.cclet.2025.111146.

References

[1] T.J. Ward, K.D. Ward, Anal. Chem. 84 (2012) 626–635.
[2] H. Lorenz, A. Seidel-Morgenstern, Angew. Chem. Int. Ed. 53 (2014) 1218–1250.
[3] J. Shen, Y. Okamoto, Chem. Rev. 116 (2016) 1094–1138.
[4] J. Sui, N. Wang, J. Wang, et al., Chem. Sci. 14 (2023) 11955–12003.
[5] V. Schurig, H.P. Nowotny, Angew. Chem. Int. Ed. 29 (1990) 939–957.
[6] X.B. Zheng, H. Zhang, Y. Zhang, et al., Anal. Chem. 88 (2016) 4955–4964.
[7] H. Li, X. Wang, C. Shi, et al., Chin. Chem. Lett. 34 (2023) 107606.
[8] D.W. Armstrong, T.J. Ward, R.D. Armstrong, et al., Science 232 (1986) 1132–1135.
[9] B. Chankvetadze, TrAC Trends Anal. Chem. 122 (2020) 115709.
[10] Y. Okamoto, E. Yashima, Angew. Chem. Int. Ed. 37 (1998) 1020–1043.
[11] S. Tang, X. Mei, W. Chen, et al., Talanta 185 (2018) 42–52.
[12] M.H. Hyun, J. Chromatogr. A 1467 (2016) 19–32.
[13] H. Frank, G.J. Nicholson, E. Bayer, J. Chromatogr. Sci. 15 (1977) 174–176.
[14] B. Huang, K. Li, Q.Y. Ma, et al., Anal. Chem. 95 (2023) 13289–13296.
[15] V. Schurig, Angew. Chem. Int. Ed. 23 (1984) 747–780.
[16] Z.Y. Gu, X.P. Yan, Angew. Chem. Int. Ed. 49 (2010) 1477–1480.
[17] Z.R. Tao, J.X. Wu, Y.J. Zhao, et al., Nat. Commun. 10 (2019) 2911.
[18] H. Jiang, K. Yang, X. Zhao, et al., J. Am. Chem. Soc. 143 (2021) 390–398.
[19] C. Liu, K. Quan, H. Li, et al., Chem. Commun. 58 (2022) 13111–13114.
[20] C. Zeng, H. Yang, M. Xu, et al., Chin. Chem. Lett. 37 (2026) 110064.

[21] C. Yuan, Z. Wang, W. Xiong, et al., J. Am. Chem. Soc. 145 (2023) 18956–18967.
[22] Y. Chen, S. Huang, L. Xia, et al., Anal. Chem. 96 (2024) 1380–1389.
[23] H.L. Qian, C.X. Yang, X.P. Yan, Nat. Commun. 7 (2016) 12104.
[24] J. Xu, G. Feng, D. Ao, et al., Adv. Mater. 36 (2024) 2406256.
[25] Y.P. Yang, J.K. Chen, P. Guo, et al., Microchim. Acta 189 (2022) 360.
[26] Y.Y. Cui, X.Q. He, C.X. Yang, et al., TrAC Trends Anal. Chem. 139 (2021) 116268.
[27] A.J. Gosselin, C.A. Rowland, E.D. Bloch, Chem. Rev. 120 (2020) 8987–9014.
[28] C. Li, Y. Wang, Y. Lu, Chin. Chem. Lett. 31 (2020) 1183–1187.
[29] S. Lee, H. Jeong, D. Nam, et al., Chem. Soc. Rev. 50 (2021) 528–555.
[30] J. Liu, Z. Wang, P. Cheng, et al., Nat. Rev. Chem. 6 (2022) 339–356.
[31] W.M. Bloch, R. Babarao, M.L. Schneider, Chem. Sci. 11 (2020) 3664–3671.
[32] G. Liu, Y.D. Yuan, J. Wang, et al., J. Am. Chem. Soc. 140 (2018) 6231–6234.
[33] K. Wu, K. Li, Y.J. Hou, et al., Nat. Commun. 7 (2016) 10487.
[34] D. Preston, J.E.M. Lewis, J.D. Crowley, J. Am. Chem. Soc. 139 (2017) 2379–2386.
[35] D.J. Bell, L.S. Natrajan, I.A. Riddell, Coord. Chem. Rev. 472 (2022) 214786.
[36] G. Wu, Y. Chen, S. Fang, et al., Angew. Chem. Int. Ed. 60 (2021) 16594–16599.
[37] Y.L. Lai, J. Su, L.X. Wu, et al., Chin. Chem. Lett. 35 (2024) 108326.
[38] D. He, L. Zhang, T. Liu, et al., Angew. Chem. Int. Ed. 61 (2022) e202202450.
[39] C. Zhu, H. Tang, K. Yang, et al., J. Am. Chem. Soc. 143 (2021) 12560–12566.
[40] Y. Li, H. Jiang, W. Zhang, et al., J. Am. Chem. Soc. 146 (2024) 3147–3159.
[41] T. Feng, X. Li, J. Wu, et al., Chin. Chem. Lett. 31 (2020) 95–98.
[42] M. Zhang, M.L. Saha, M. Wang, et al., J. Am. Chem. Soc. 139 (2017) 5067–5074.
[43] N. Ahmad, H.A. Younus, A.H. Chughtai, et al., Chem. Soc. Rev. 44 (2015) 9–25.
[44] S.M. Xie, N. Fu, L. Li, B.Y. Yuan, et al., Anal. Chem. 90 (2018) 9182–9188.
[45] B. Tang, X. Zhang, L. Geng, et al., J. Chromatogr. A 1636 (2021) 461792.
[46] Z.H. Luo, Y.L. Zhu, X.Y. Ran, Talanta 277 (2024) 126388.
[47] A.C. Eaby, D.C. Myburgh, A. Kosimov, et al., Nature 616 (2023) 288–292.
[48] D. He, H. Ji, T. Liu, et al., J. Am. Chem. Soc. 146 (2024) 17438–17445.
[49] H. Liu, J. Chen, M. Chen, et al., Anal. Chim. Acta 1274 (2023) 341496.
[50] J. Zhou, J. Tang, W. Tang, TrAC-Trends Anal. Chem. 65 (2015) 22–29.
[51] X. Li, X. Jin, X. Yao, et al., J. Chromatogr. A 1467 (2016) 279–287.
[52] H. Zhou, J. Chen, H. Li, et al., Talanta 211 (2020) 120743.